Taiwania 66(2): 165–173, **2021**
DOI: 10.6165/tai.2021.66.165

Genetic diversity of *Cyclina sinensis* (Veneridae): Resource management in Taiwan

Kui-Ching HSU[1], Hsin-Ju WU[1], Po-Hsun KUO[2], Yuh-Wen CHIU[1,*]

1. Department of Biological Resources, National Chiayi University, Chiayi 60004, Taiwan.
2. Department of Industrial Management, National Taiwan University of Science and Technology, Taipei 10607, Taiwan.
[*]Corresponding author's E-mail: chiuywlab@gmail.com

(Manuscript received 6 October 2020; Accepted 21 March 2021; Online published 15 April 2021)

ABSTRACT: Artificial breeding of the iron clam, *Cyclina sinensis,* was successful for the first time in Taiwan in 2020. To prevent potential inbreeding depression and genetic incompatibility, the genetic diversity and structure of wild populations of *C. sinensis* must be assessed. The genetic diversity of 153 iron clams from 7 sample populations in Taiwan, including the Penghu and Kinmen Islands, was examined in this study. A total of 658 base pairs in the mitochondrial DNA cytochrome c oxidase subunit I sequence revealed only one phylogenetically informative site, and 15 haplotypes were identified. Compared with populations on the Chinese coast, those in the south of and in Taiwan Strait exhibited much lower nucleotide diversity (0.0003 vs. 0.0022), which may cause difficulties in the artificial breeding of *C. sinensis* in Taiwan. Compared with other bivalves, the *C. sinensis* of northern China did not exhibit lower nucleotide diversity (0.0022 vs. 0.002–0.006). Demographic analyses of *C. sinensis* in East Asia revealed no pattern of decline. Although Taiwan is closer to southern China (F_{ST} = 0.000), the introduction of broodstock from northern China should be evaluated for viability. In addition, our study revealed a difference in the genetic composition and genetic diversity of *C. sinensis* in Taijiang National Park before and after the enactment of the annual catch limit policy, which warrants further study.

KEY WORDS: *Cyclina sinensis*, Taiwan, cytochrome c oxidase subunit I, genetic diversity, genetic structure.

INTRODUCTION

The bivalve *Cyclina sinensis* (Gmelin, 1791) belongs to the family Veneridae and is one of the most economically important shellfish. This species is widely distributed on the flat coasts of East Asia, inhabiting various environments from muddy sand beaches to estuaries. It tolerates a wide range of salinity levels (5‰–35‰, with an optimum of 15‰–25‰) and temperatures (−2°C–33°C, with an optimum of 20°C–25°C; Wang *et al.*, 1993, 2008). *Cyclina sinensis* is considered a rich source of protein and polysaccharides (Li *et al.*, 2010) and a key ingredient of Chinese medicine (Dong *et al.*, 2016). Researchers have isolated certain peptides that might be beneficial for antioxidation and immunomodulation (Li *et al.*, 2019; Jiang *et al.*, 2020). However, due to their overexploitation and the deterioration of their habitats in recent decades, wild *C. sinensis* populations have experienced considerable decline (Yang *et al.*, 2004). Thus, an artificial breeding program has been in progress, with broodstock depending almost wholly on wild resources (Zhao *et al.*, 2009).

In Taiwan, *C. sinensis* used to be abundant on the west coast, but the species population has been greatly reduced in the last 20 years. Taiwan has a long coastline, and aquaculture is vital to the economies of coastal regions (Chen, 1990). In 2020, the artificial breeding of *C. sinensis* was successful for the first time in Taiwan (Council of Agriculture, 2020). Although aquaculture systems in Taiwan are well established, they still encounter problems, such as the loss of genetic variation that may result in inbreeding depression (Allendorf and Phelps, 1980). Among the shellfish cultivated through Taiwanese aquaculture, the spotted hard clam (*Meretrix petechialis*) is the most numerous of the shellfish (Chen and Ho, 2001), with mass mortality occurring in *M. petechialis* farms. Huang *et al.* (2020) reported that the genetic diversity of cultivated hard clams in Taiwan is much lower than that of cultured clams from the Chinese coast. Thus, the genetic diversity and structure of wild populations must be examined to avoid inbreeding depression and genetic incompatibility. This study investigated the genetic diversity of *C. sinensis* in Taiwan and analyzed the genetic structure of *C. sinensis* in East Asia. On the basis of these results, we offer suggestions for the introduction of broodstock to the artificial breeding of *C. sinensis*.

In 2009, Taijiang National Park was established in southwestern Taiwan to protect the biodiversity and natural resources of wetland ecosystems. In 2012, a limit was placed on the total annual capture fisheries production of *C. sinensis*. Our study obtained specimens of *C. sinensis* from Taijiang National Park in 2011 and again in 2012, which was the first year of the capture fisheries production policy. Thus, we could compare the genetic composition and genetic diversity of these two groups of *C. sinensis* (2011 and 2012) to evaluate the effects of the annual catch limit policy.

The mitochondrial DNA (mtDNA) cytochrome c oxidase subunit I (COI) gene was used to investigate the genetic diversity and structure of *C. sinensis*. MtDNA

sequences are usually analyzed in studies of animal phylogeography, and among all mtDNA genes, COI is a widely accepted marker for evaluating levels of genetic diversity and differentiation (Yang *et al.*, 2016; Chiu *et al.*, 2017; Han *et al.*, 2019).

MATERIALS AND METHODS

Specimens and COI sequence collection

A total of 133 *C. sinensis* specimens were collected from 7 locations between July and September 2011. The sample sites consisted of wetlands and lagoons in the following three locations: Taiwan [Danshuei (DS), Nanliao (NL), Lukang (LK), Taijiang (TJ) and Dongkang (DK)], the Penghu Islands (PH), and the Kinmen (KM) Islands (Table 1 and Fig. 1). At the TJ sample site, we compared the genetic diversity of *C. sinensis* not only with that of other sample sites but also within the site over 2 years. Thus, the sampling procedure at the TJ site differed from that of the other sample sites. Twenty specimens were collected in September 2012 in the TJ site again (TJb and 2011 as TJa) (Table 1). Moreover, the mean total shell length in each of the five age cohorts was 1.45–2.10 (one year), 2.50–3.20 (2 years), 3.50–3.80 (3 years), 4.00–4.80 (4 years), and 4.50–5.00 (> 4 years) cm (Yu and Zheng, 1995). The commercial shell length is 3–4 cm (Zhao *et al.,* 2009). In TJ, the total shell length of each specimen was measured using vernier calipers, and we analyzed only specimens less than 1 year old (total shell length < 1.4 cm). For the other sample sites, we did not measure the total shell length. We analyzed specimens of all sizes and randomly sampled 20 specimens. At the Danshuei (DS) site, we obtained only 13 specimens.

Genomic DNA extracted from muscle tissue by a Tissue & Cell Genomic DNA Purification Kit (GeneMark-DP021). The COI gene was amplified by polymerase chain reaction (PCR) using the primers LCO-1490 (5'-GGTCAACAAATCATAAAGATATTGG-3') and HCO-2198 (5'-TAAACTTAGGGTGACCAAAAATC-3') (Folmer *et al.*, 1994). Each 50 µl PCR reaction mixture contained 5 ng of template DNA, 5 µl of 10x reaction buffer, 4 µl of dNTP mix (10 mM), 5 pmol of each primer and 2U of Taq polymerase (TaKaRa, Taq polymerase). The PCR was programmed on an MJ Thermal Cycler as first denaturation at 94°C for 3 min, 40 cycles of denaturation at 94°C for 30 s, annealing at 50°C for 40 s and extension at 72°C for 1 min 30 s, followed by a 72°C extension for 10 min and 4°C for storage. The purified PCR products were sequenced using an ABI 377 automated sequencer (Applied Biosystems, Foster City, CA, USA). The chromatograms were checked with the CHROMAS software (Technelysium), and the sequences were manually edited using BIOEDIT 6.0.7 (Hall, 1999). Besides, the sequences of *C. sinensis* in the coastline of China and Japan from the previous studies (Chen *et al.*, 2011; Ni *et al.*, 2012) were download from GenBank (GU078392-429; HM021146-49; HQ703115-31).

Data analysis

The nucleotide sequences were aligned in Clustal X 1.81 (Thompson *et al.*, 1997). The selection of the best-fit nucleotide substitution models was performed using the Bayesian information criterion (BIC) in jModelTest 2.0 (Darriba *et al.*, 2012). The most appropriate nucleotide substitution model was HKY. The intra-population genetic diversity levels were estimated using haplotype diversity (*h*) (Nei and Tajima, 1983) and nucleotide diversity (θ_π) (Nei, 1987) indices in DnaSP v5 (Librado and Rozas, 2009). Moreover, our study also estimated another genetic diversity index, θ_ω. The current genetic diversity estimates (θ_π) were based on the pairwise differences between the sequences, and the historical diversity estimates (θ_ω) were based on the number of segregating sites among the sequences. Comparing the estimates generated by these two indices provides insight into the population dynamics over recent evolutionary history (Templeton, 1993). Pairwise F_{ST} values were used to examine the spatial partitioning of genetic variation among populations by DnaSP. Pairwise K2P distance (Kimura 2 parameter) was estimated by MEGA -X (Kumar *et al.*, 2018). The median-joining algorithm (Bandelt *et al.,* 1999) from Network 5.0 was used to reconstruct the haplotype networks.

The degree of genetic differentiation (pairwise F_{ST} values) among populations and analyses of molecular variance (AMOVA) were performed in Arlequin v3.5 (Excoffier and Lischer, 2010). AMOVA partitioning was used to observe the within-population (F_{ST}), within-group (F_{SC}), and among-group (F_{CT}) components of the variation among samples. The population clusters were estimated based on $Ø_{CT}$ values using SAMOVA1.0 (Dupanloup *et al.*, 2002). The test was performed with K-values of 2-6, and the value for which $Ø_{CT}$ was highest was chosen as the best grouping. Genetic connectivity among the populations was assessed using the Bayesian MCMC method implemented in MIGRATE-N 4.4.3 (Beerli, 2016). MIGRATE-N estimates the mutation-scaled population size ($\theta = 2Ne\mu$ for haploid mtDNA) for each locality and the mutation-scaled immigration rate ($M= m/\mu$), where Ne is the effective population size, µ is the mutation rate of loci per generation, and m is the immigration rate per generation. The effective number of immigrants per generation was calculated for haploid data with female-transmission following the equation $Nm = \theta \times M$. The runs consisted of two replicates of 10 short chains and three long chains, with the first 10,000 genealogies discarded.

The historical demographic expansions were examined using several different methods. The effective

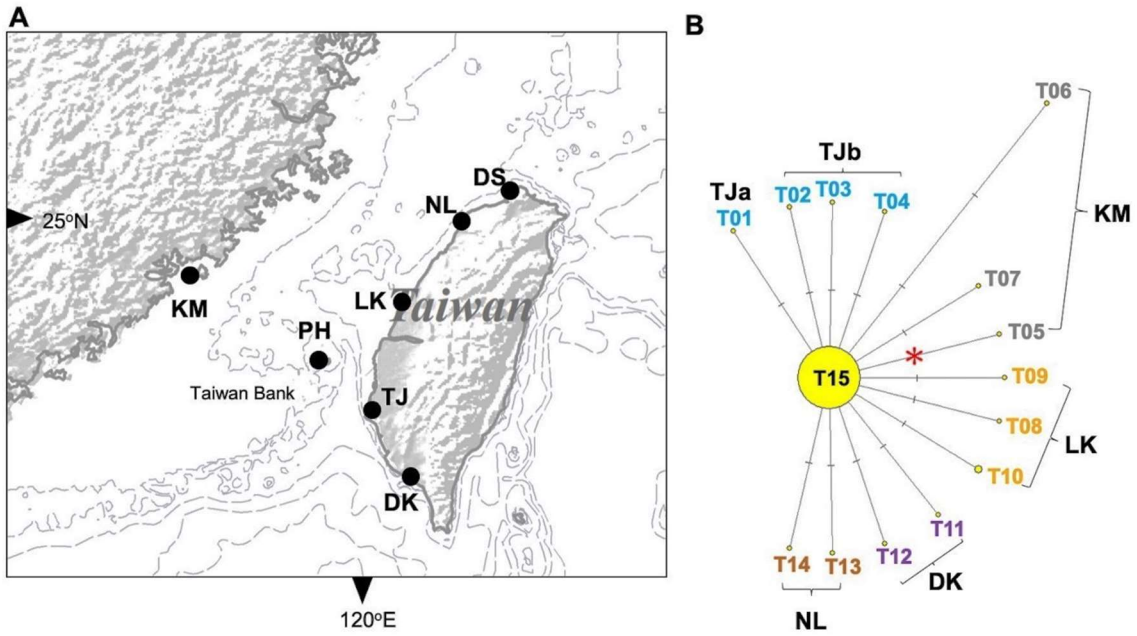

Fig. 1. A: The seven sampling localities of *Cyclina sinensis* are indicated by •. Refer to Table 1 for the abbreviations of localities. **B**: The haplotype network of *C. sinensis* in the present study based on the COI sequences. The phylogenetic informative and variation sites between haplotypes are indicated by * and -.

Table 1. Samples of used for mtDNA analysis, location, code and summary statistics. N, number of specimens; S, number of polymorphism sites; Hd, haplotype diversity; θ_π and θ_ω, nucleotide diversity; h, number of haplotypes.

	Code	N	S	haplotype	Hd	θ_π	θ_ω
Danshuei	DS	13	0	T15	0.000	0.0000	0.0000
Nanliao	NL	20	2	T13,T14,T15	0.195	0.0003	0.0009
Lukang	LK	20	3	T08,T09,T10,T15	0.284	0.0005	0.0013
Taijiang	TJ	40	4	T01,T02,T03,T04,T15	0.195	0.0003	0.0014
2011	TJa	20	1	T1,T15	0.100	0.0002	0.0004
2012	TJb	20	3	T02,T03,T04,T15	0.284	0.0005	0.0013
Dongkang	DK	20	2	T11,T12,T15	0.195	0.0003	0.0009
Penghu	PH	20	0	T15	0.000	0.0000	0.0000
Kinmen	KM	20	4	T05,T06,T07,T15	0.363	0.0007	0.0017
Taiwan		153	16	15	0.187	0.0003	0.0041

population size changes over time were evaluated using the Bayesian Skyline Plots (BSP) in BEAST v1.8.0 with 10^7 MCMC steps and the first 10% as burn-in (Drummond *et al.*, 2013). A strict clock model with a Bayesian Skyline tree was used, and ran 10^6 generations. A mutation rate of 1.56% per million years (myr) has been calibrated for the mtDNA COI gene in freshwater snail *Semisulcospira libertine* (Hsu *et al.*, 2014) because of the lack of a calibrate point. Ni *et al.* (2012) used a range of divergence rates of COI for bivalve Arcidae (0.7% Myr^{-1}) (Marko, 2002) and gastropod teguline (2.4% Myr^{-1}) (Hellberg and Vacquie, 1999) to generate a time frame for the lineage divergence of *C. sinensis* in China. Plots for each analysis were drawn using Tracer v1.5 (Rambaut *et al.*, 2013). The demographic analyses, Tajima's *D* (Tajima, 1989), Fu's *F*s (Fu, 1997) and Ramos-Onsins and Rozas' R_2 (Ramos-Onsins and Rozas, 2002) tests, and the mismatch distribution analyses implemented in DnaSP. Under a population expansion model, significant negative values of Tajima's *D* and Fu's F_S and small positive values of R_2 were expected.

RESULTS

Genetic diversity in Taiwan

A total of 658 base pairs (bp) of mtDNA COI sequences from 153 specimens in 7 sampling populations were analyzed (Table 1, Fig. 1A). The sequences were unambiguously aligned with no indels. A total of 15 haplotypes (15 variable sites [singletons]) and only one phylogenetically informative site (GenBank accession number: MW387516–MW387530) were obtained. Among the 15 haplotypes, only one (T15) was shared among all populations (Table 1, Fig. 1B). The populations of KM, LK, and TJb (TJ in 2012) had the most private haplotypes, and the populations of DS and PH had only one haplotype (T15). At the TJ sample site, the TJa (2011) and TJb (2012) populations shared only one haplotype (T15; Table 1, Fig. 1B). Haplotype T15 was located in the interior of the haplotype network, and the other haplotypes were all located in the tips (Fig. 1B). Only one phylogenetically informative site was identified between haplotype T15 and T05, whereas haplotype T05 was only distributed in the population in KM (Table 1, Fig. 1B).

The mean mtDNA haplotype diversity across all sampled populations was 0.176 (range: 0.000–0.363; Table 1). The mean mtDNA nucleotide diversity (θ_π) across all sampled populations was 0.0003 (range: 0.0000–0.0007). In the total sample, the haplotype diversity was 0.187

Table 2. Matrix of pairwise F_{ST} (above) and K2P distance (below) based on mtDNA data. Refer to Table 1 for the abbreviations of localities. Values were significantly different from zero (p = 0.05) are marked with an asterisk (*).

	DS	NL	LK	TJ	TJa	TJb	DK	PH	KM
DS		0.000	0.000	0.000	0.000	0.000	0.000	0.000	0.021*
NL	0.015		0.000	0.000	0.000	0.000	0.000	0.000	0.015*
LK	0.023	0.038		0.000	0.000	0.000	0.000	0.000	0.013*
TJ	0.015	0.030	0.038		-	-	0.000	0.000	0.015*
TJa	0.008	0.023	0.030	-		0.000	0.000	0.000	0.018*
TJb	0.023	0.038	0.046	-	0.030		0.000	0.000	0.013*
DK	0.015	0.030	0.038	0.030	0.023	0.038		0.000	0.015*
PH	0.000	0.015	0.023	0.015	0.008	0.023	0.015		0.021*
KM	0.038	0.053	0.061	0.053	0.046	0.061	0.053	0.038	

Table 3. Results of SAMOVA tests for increasing K (number of groups) values. See Table 1 for the locality codes.

No. of groups	Groupings	$Ø_{CT}$	% Variance among groups
2	(DS) (DK,KM,LK,NL,PH,TJ)	0.000	0
3	(NL) (DK,DS,LK,PH,TJ) (KM)	0.040	3.99
4	(DK,PH,TJ) (DS,NL) (LK) (KM)	0.033	3.33
5	(LK) (PH,TJ) (DS,NL) (KM) (DK)	0.039	3.89
6	(DK) (KM) (DS) (LK) (NL) (PH,TJ)	0.032	3.22

and the nucleotide diversity was 0.0003. The pairwise F_{ST} values were nearly 0.000, excluding the F_{ST} values between the KM population and others, which ranged from 0.013 to 0.021 (Table 2). The K2P pairwise distances ranged from 0.000 (between the DS and PH populations) to 0.061 (between the KM and LK populations; Table 2). The K2P distance between TJa and TJb was 0.030.

In the SAMOVA analysis, the highest $Ø_{CT}$ value (0.040) occurred at K = 3, with a grouping arrangement of NL, DK + DS + LK + PH + TJ, and KM (Table 3). The Analysis of Molecular Variance (AMOVA) results indicated no significant genetic structure at several levels based on the geographical, SAMOVA and sampling years (Table 4). Partitioning of genetic diversity based on four groups (scheme 6) revealed the following division of the population groups: (scheme 6) NL, DK + DS + LK + PH + TJa, TJb, and KM. A comparison of all scenarios indicated that the samples from TJb were different from TJa and the other samples (Table 4).

Genetic diversity in East Asia

From Chen *et al.* (2011) and Ni *et al.* (2012), we obtained the data of all mtDNA COI sequences of *C. sinensis* from the Chinese coastline and Japan. After alignment, a total of 417 bp of mtDNA COI sequences were analyzed. The sample sites consisted of four regions (Fig 2): Japan (brown), northern China (yellow), southern China (purple), and Taiwan (blue). The haplotypes of both northern and southern China were distributed in the Taiwan Strait (Ni *et al.*, 2012). A total of 74 sequences

Table 4. Analysis of molecular variance (AMOVA) for *Cyclina sinensis*.

Scheme Category description	% Var.	Statistic	p
1. Two groups: (KM) (DS,NL,LK,TJ,DK,PH)			
Among groups	6.31	F_{SC}=-0.014	<0.889
Among populations in group	-1.30	F_{ST}=0.050	<0.191
Within population	94.99	F_{CT}=0.063	<0.117
2. Three groups: (KM) (PH)(DS,NL,LK,TJ,DK)			
Among groups	2.24	F_{SC} =-0.007	<0.835
Among populations in group	-0.70	F_{ST} =0.015	<0.215
Within population	98.46	F_{CT} =0.022	<0278
3. Three groups: (KM) (DK) (PH,DS,NL,LK,TJ)			
Among groups	3.99	F_{SC} =-0.017	<0.910
Among populations in group	-1.58	F_{ST} =0.024	<0.224
Within population	97.59	F_{CT} =0.040	<0.151
4. Four groups: (KM) (DK) (NL) (PH,DS,LK,TJ)			
Among groups	3.50	F_{SC} =-0.021	<0.927
Among populations in group	-1.99	F_{ST} =0.015	<0.227
Within population	98.49	F_{CT} =0.035	<0.118
5. Three SAMOVA groups: (NL) (KM) (PH,DS,LK,TJ,DK)			
Among groups	3.99	F_{SC} =-0.016	<0.902
Among populations in group	-1.58	F_{ST} =0.024	<0.218
Within population	97.59	F_{CT} =0.040	<0.134
6. Four groups: (NL) (KM) (PH,DS,LK,TJa,DK) (TJb)			
Among groups	**4.54**	F_{SC} =-0.031	<1.000
Among populations in group	-2.93	F_{ST} =0.016	<0.170
Within population	98.39	F_{CT} =0.045	<0.090
A. Two groups: (Japan) (North Sea, South Sea, Taiwan)			
Among groups	**78.16**	F_{SC} =0.327	<0.001
Among populations in group	7.13	F_{ST} =0.853	<0.001
Within population	14.71	F_{CT} =0.782	<0.261
B. Three groups: (Japan) (North Sea, South Sea) (Taiwan)			
Among groups	42.79	F_{SC} =0.349	<0.001
Among populations in group	19.98	F_{ST} =0.628	<0.001
Within population	37.22	F_{CT} =0.428	<0.488
C. Three groups: (Japan) (South Sea) (North Sea, Taiwan)			
Among groups	44.86	F_{SC} =0.355	<0.001
Among populations in group	19.59	F_{ST} =0.645	<0.001
Within population	35.55	F_{CT} =0.449	<0.342
D. Three groups: (Japan) (North Sea) (South Sea, Taiwan)			
Among groups	60.62	F_{SC} =-0.053	<0.998
Among populations in group	-2.08	F_{ST} =0.585	<0.001
Within population	41.47	F_{CT} =0.606	<0.169

were collected and 35 haplotypes were identified. The pairwise F_{ST} among these four regions ranged from 0.042 (between Taiwan and southern China) to 0.913 (between southern China and Japan). The F_{ST} values between northern China and Taiwan and between northern China and southern China were 0.346 and 0.387, respectively. The mean F_{ST} between Japan and other regions was 0.896.

Among the 35 haplotypes, Taiwan and southern China shared 3 (S1–S3); Taiwan, northern China, and southern China shared 1 (S4); and Taiwan and northern China shared 1 (S5; Fig. 2). The haplotype S4 was distributed from Hainan Island to Shanghai (south of Yangtze River), and the haplotype S5 was distributed in and north of the Taiwan Strait. The haplotype network

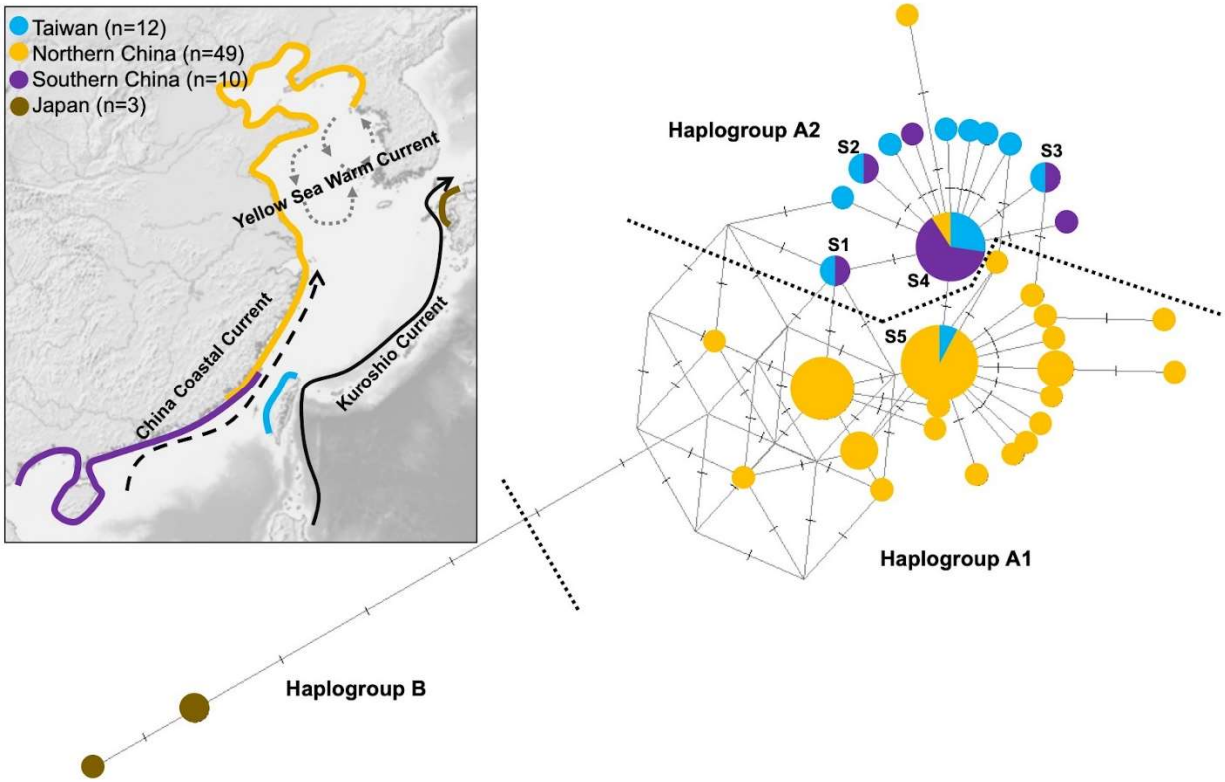

Fig. 2. The COI haplotype network of *Cyclina sinensis* in East Asia. All samples were assorted as four groups, northern China coast (Yellow), southern China coast (Purple), Taiwan (Blue), and Japan (Brown).

indicated that these 35 haplotypes could be classified into 2 haplogroups, with haplogroup A being distributed in northern China, southern China, and Taiwan and haplogroup B being distributed in Japan. Haplogroup A could be divided into subgroups A1 and A2. Haplogroup A2 was almost completely distributed in southern China and Taiwan, and haplogroup A1 was almost solely distributed in northern China. The K2P distance between haplogroups A and B was 0.025, and the K2P distances within the haplogroups were 0.005 and 0.002, respectively. Upon AMOVA analysis, the partitioning of genetic diversity based on the two groups (scheme A) revealed that all populations were divided into two groups: Japan and northern China, southern China, and Taiwan (Table 4).

The effective population size in each population and the migration number (per generation) were analyzed using MIGRATE-N. Northern China had the largest effective population size (θ_N = 0.00097 [95% CI: 0.00060–0.00160]; Fig. 3). Migration was most frequent between northern China and Japan (Nm_{N-J} = 0.930). Japan had the most immigration, and most immigrants were from northern China (Fig. 3). Southern China had the least immigration. Northern China had the most emigration, and the values for emigration number (per generation) from Taiwan to Japan, northern China, and southern China were 0.267, 0.287, and 0.296, respectively (Fig. 3).

Bayesian skyline plots, which simulate the fluctuations

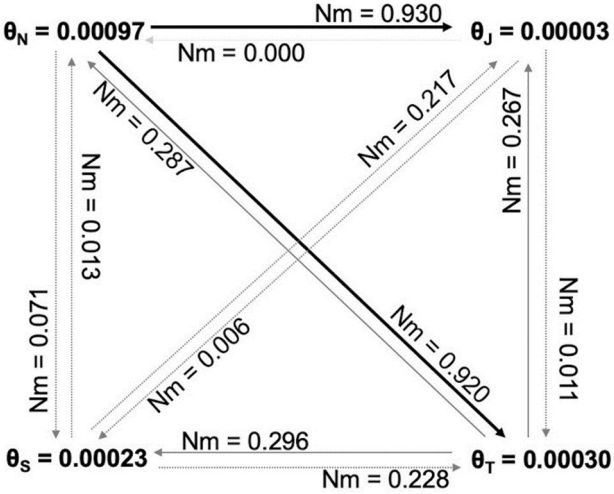

Fig. 3. Number of migrants (per generation, Nm) among *Cyclina sinensis* groups from northern China (N), southern China (S), Taiwan (T), and Japan(J), and their effective population sizes (θ).

in population size over time, indicated that the population size of *C. sinensis* in East Asia is in contraction in the lest 5,000 years (Fig. 4A). The mismatch distribution did not fit the sudden expansion model (bimodal, $P > 0.05$; Fig. 4B). However, the signature of a recent demographic expansion was detected in Tajima's *D* test (−1.9513, $P < 0.05$), Fu's F_s test (−36.719, $P < 0.001$), and an R_2 (0.0366) test (Fig. 4B).

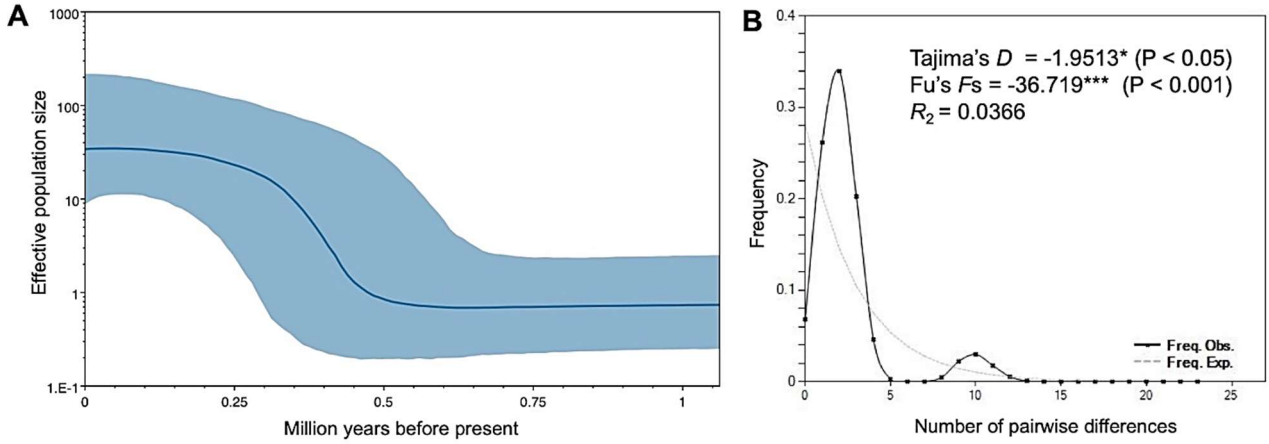

Fig. 4. A: Bayesian skyline plot of *Cyclina sinensis* in East Asia. Time is reported on the x-axis as MYR (millions years ago). Effective population size is reported on the y-axis. Blue lines represent the median estimates of effective population size, while colored area represent the upper and lower 95% highest posterior density limits. **B**: Mismatch distribution analysis shows bimodal distribution. The observed (black solid line) and expected (gray dotted line) mismatch distributions. Number of differences and frequency are reported on the x-axis and y-axis.

DISCUSSION

Genetic diversity

Compared with the genetic diversity of the spotted hard clam in Taiwan (Huang *et al.*, 2020), the genetic diversity of *C. sinensis* in Taiwan is very low (θ_π in COI gene, *C. sinensis* = 0.0003; *M. petechialis* = 0.0029). In Taiwan, the genetic diversity of *C. sinensis* was lower than that of both the wild and cultured populations of *M. petechialis* (0.0011). We questioned whether bias was present in our samples. Ni *et al.* (2012) indicated that the nucleotide diversity in 21 populations of *C. sinensis* along the Chinese coast ranged from 0.0000 to 0.0044, and that in Xiamen was 0.0007. Xiamen is located 15 km from the island of Kinmen, where the nucleotide diversity was also 0.0007 (Table 1). Thus, the low genetic diversity of *C. sinensis* in Taiwan is not because of our small sample size.

Ni *et al.* (2012) obtained 335 specimens from 21 locations in East Asia and revealed a markedly low nucleotide diversity in 4 locations in the Taiwan Strait and South China Sea, namely Xiamen, Maoming, Beihai, and Saya (mean θ_π = 0.000275; 0.0000–0.0007). This θ_π was equal to that in Taiwan (Table 1). However, the mean θ_π in 16 other locations in northern China was 0.0022, and that in Japan was 0.0030. Thus, the intraspecific genetic diversity of *C. sinensis* in East Asia was not low; in fact, it was much lower in most populations in the south of the Taiwan Strait. We subsequently investigated whether the "natural" nucleotide diversity of *C. sinensis* in the south of and in Taiwan Strait was lower than that in other regions. For example, the environmental factors, e.g. sea water temperature, in South China Sea did not suit *C. sinensis*. In a previous study (Ni *et al.*, 2012), the θ_π in Dongxing, in the Beibu Gulf near Vietnam, was 0.0011. Thus, the natural environmental factors did not result in the lower nucleotide diversity of *C. sinensis* in the South China Sea.

Based on data sets of the COI gene in other bivalves, our study recorded that the values of θ_π for *M. petechialis* (Veneridae, see Huang *et al.*, 2020) in Taiwan, *Tridacna maxima* (Cardiidae, see Othmen *et al.*, 2020) in the Red Sea, *Atrina pectinata* (Pinnidae, see Xue *et al.*, 2014) along the coast of China, and *Ruditapes decussatus* (Veneridae, see Sanna *et al.*, 2017) in the western Mediterranean are 0.0029, 0.004, 0.002–0.006, and 0.0048, respectively. The mean θ_π of *C. sinensis* in the north of the Taiwan Strait is 0.0022 (Ni *et al.*, 2012). Thus, the population genetic diversity is low in the south of the Taiwan Strait, but not in East Asia. Although the demographic analyses of *C. sinensis* in East Asia did not indicate a pattern of population decline (Fig. 4), our findings suggest that the population size in the South China Sea and the Taiwan Strait has declined. This low genetic diversity may be caused by overexploitation and habitat deterioration in recent decades (Yang *et al.*, 2004).

Genetic structure

The average planktonic larval duration of *C. sinensis* is 7 days, which is relatively short (Zeng and Li, 1991). *C. sinensis* adults migrate no more than 80 meters (Pan *et al.*, 2005), this species is suitable for investigations of the interactions of various factors on genetic structure. In the present study, the haplotype network of all sequences in East Asia demonstrated that the populations could be divided into three metapopulations; Japan, northern China, and southern China (Fig. 2). The southern China metapopulation includes the island of Taiwan. These results are consistent with those in Ni *et al.* (2012). Moreover, this intraspecific genetic structure is the same as those for many sympatric animals, such as *Chelon haematocheilus* (fish, Liu *et al.*, 2007), *Atrina pectinata* (mollusk, Liu *et al.*, 2011), and *Eriocheir sensu stricto*

(crustacean, Xu *et al.*, 2009). Previous studies (Liu *et al.*, 2007, 2011; Xu *et al.*, 2009; Ni *et al.*, 2014) have proposed that during the Pleistocene glaciations, the Taiwan Strait and Tsushima Strait exposed and isolated the migrations of marine species. The spatial structure of the phylogeography of the Northwestern Pacific encompassed three regions: the East China Sea, the South China Sea, and the Sea of Japan (Fig. 2). Over time, genetic differentiations occurred among populations. Yan *et al.* (2020) reported that the mismatch distribution of *Scatophagus argus* in the South China Sea appeared bimodal because two highly divergent lineages were present. The mismatch distribution in our study also appeared bimodal because we observed divergences among three metapopulations of *C. sinensis* (Fig. 4B).

After glaciation, the isolations disappeared and oceanographic current systems shaped the migrations of marine species (Shen *et al.*, 2011; He *et al.*, 2015). Migrations from northern China to Japan occurred the most frequently (Nm = 0.930; Fig. 3). Migrations from northern China to Taiwan were also high (Nm = 0.920), but migrations from northern China to southern China were low (Nm = 0.071). Our study suggests the migrations were shaped by the Yellow Sea Warm Current (Fig. 2). Our research demonstrated that the haplotype S5 (northern China group) was distributed north of the Taiwan Strait (Fig. 2). Differences in the seafloor topography and ocean conditions in the north and south of the Taiwan Strait (South and East China Seas) were likely the reason why the northern lineage did not migrate southward through the Taiwan Strait. The East China Sea is a flat and relatively isolated region, and the Taiwan Bank acts as the boundary between the Taiwan Strait and the South China Sea (Liao *et al.*, 2008; Jiang *et al.*, 2011). Thus, the cyclical migrations were limited to within the Yellow and East China Sea.

The haplotype S4 (southern China group) was distributed from Hainan Island to Shanghai (south of the Yangtze River; Fig. 2). The Yangtze River (also known as the Changjiang River) is the third largest river in the world. The large freshwater outflow has been assumed by researchers to be a major barrier limiting the gene flow of coastal species, including the gastropod *Cellana toreuma* (Dong *et al.*, 2012) and two varieties of *Sargassum* (Cheang *et al.*, 2010). Additionally, the China Coastal Current flows from the South China Sea northward. The main breeding season of *C. sinensis* is from July to September (Ni *et al.*, 2012) and during this period, the northward China Coastal Current is weakened. Our findings suggest that the smaller effective population size in southern China (Fig. 3) and the weaker ocean current resulted in fewer northward migrations.

Resource and broodstock management

Our results demonstrate that the populations in Taiwan were more closely related to the populations in southern China than to those in northern China (Fig. 2). These results concur with those of studies on whiskered velvet shrimp (*Metapenaeopsis barbata*; Chu *et al.*, 2012) and *M. petechialis* (Huang *et al.*, 2020). As proposed by Huang *et al.* (2020), broodstock from southern China may facilitate the management of genetic diversity in cultivated *C. sinensis* in Taiwan to prevent genetic incompatibility. However, our study found that the diversity and effective population size of *C. sinensis* in southern China were very low (Fig. 3; Ni *et al.*, 2012). Thus, the results do not support the introduction of *C. sinensis* broodstock from southern China. Moreover, we demonstrated that northern China and Taiwan have two shared haplotypes (S4 and S5, Fig. 2). Thus, broodstock from northern China should be more closely evaluated.

In 2009, Taijiang National Park was established to protect the biodiversity in wetland ecosystems. This national park works to protect the habitats of *Platalea minor*. In 2012, the park implemented a policy limiting the capture of *C. sinensis*. At this sample site, we analyzed specimens less than 1 year old (total shell length < 1.4 cm; Yu and Zheng, 1995). At other sample sites, the specimen sizes varied. Thus, we found that the haplotype and nucleotide diversities in the TJa sample (2011) were smaller than those at other sites, although the haplotype and nucleotide diversities in sample sites DS and PH were both zero (Table 1). The sampling of *C. sinensis* specimens in DS and PH was undertaken with difficultly and may explain the low diversity in these two sample sites (Table 1).

To evaluate the effects of the capture limit policy, we examined *C. sinensis* again in 2012 (TJb). The genetic composition and genetic diversity in TJb were different from that of TJa (Tables 1, 2, and 4). Compared with TJa, the diversity in TJb was higher (Table 1), the K2P distance between TJb and other samples was higher than that between TJa and other samples, and the AMOVA analysis revealed higher variations among groups when TJb was as a single group (schemes 5 and 6; Table 4). The annual catch limit policy seems to be effective, but further evaluation is warranted. We intend to reexamine the genetic diversity of *C. sinensis* in TJ and contribute further resource material for future studies.

CONCLUSION

The present study revealed that the genetic diversity of *C. sinensis* was low in southern China, including the island of Taiwan. Regarding the resource management of *C. sinensis* in Taiwan, we propose three policies. First, for in situ conservation, the populations of Kinmen Island and Taiwan Island may be considered two different management units. Second, the artificial breeding of *C. sinensis* in Taiwan must be carefully evaluated, and if artificial breeding is employed, our data suggest the introduction of broodstock from northern China. Third,

the annual catch limit policy appears to be effective, but further evaluation is required. The results of this research are valuable for future evaluations of the resource management and conservation of *C. sinensis*.

ACKNOWLEDGMENTS

This work is supported by Taijiang National Park, Tainan 70955, Taiwan. This work was financially supported by the "Center for Cyber-Physical System Innovation" from The Featured Areas Research Center Program within the framework of the Higher Education Sprout Project by the Ministry of Education (MOE) in Taiwan. We also thank the anonymous reviewers and associate editor for their helpful comments. This manuscript was edited by Wallace Academic Editing.

LITERATURE CITED

Allendorf, F.W. and S.R. Phelps. 1980. Loss of genetic variation in a hatchery stock of cutthroat trout. Trans. Am. Fish. Soc. **109(5)**: 537–543.

Bandelt, H.J., P. Forster and A. Röhl. 1999. Median-joining networks for inferring intraspecific phylogenies. Mol. Biol. Evol. **16(1)**: 37–48.

Beerli, P. 2016. MIGRATE-N 4.4.3. https: peterbeerli.com/migrate/tutorials.html.

Cheang, C.C., K.H. Chu and P.O. Ang Jr. 2010. Phylogeography of the marine macroalga *Sargassum hemiphyllum* (Phaeophyceae, Heterokontophyta) in northwestern Pacific. Mol. Ecol. **19(14)**: 2933–2948.

Chen, H.Y and Y.D. Ho. 2001. Production of hard clam seed. In G. F. Liu (Ed.), Breeding and aquaculture techniques for fishes and clams in southwestern Taiwan, (pp. 81–109). Yunlin, Taiwan: Taishi Branch, Fisheries Research Institute, Council of Agriculture (in Chinese).

Chen, J., Q. Li, L. Kong and H. Yu. 2011. How DNA barcodes complement taxonomy and explore species diversity: the case study of a poorly understood marine fauna. PLOS one **6(6)**: e21326.

Chen, L.C. 1990. Aquaculture in Taiwan. Oxford, UK: Blackwell Scientific Publications.

Chiu, Y.W., H. Bor, P.H. Kuo, K.C. Hsu, M.S. Tan, W.K. Wang and H.D. Lin. 2017. Origins of *Semisulcospira libertina* (Gastropoda: Semisulcospiridae) in Taiwan. Mitochondrial DNA. A **28(4)**: 518–525.

Chu, T.J., D. Wang, H.L. Huang, F.J. Lin and T.D. Tzeng. 2012. Population structure and historical demography of the whiskered velvet shrimp (*Metapenaeopsis barbata*) off China and Taiwan inferred from the mitochondrial control region. Zool. Stud. **51**: 99–107.

Council of Agriculture. 2020. Artificial breeding of *Cyclina sinensis* succeeded. https://www.tfrin.gov.tw/News_Content.aspx?n=241&sms=9046&s=233525.

Darriba, D., G.L. Taboada, R. Doallo and D. Posada. 2012. jModelTest 2: more models, new heuristics and parallel computing. Nat. Methods **9(8)**: 772.

Dong, P., G. Ma, L. Chang, Y. Zhu and X. Tian. 2016. The complete mitochondrial genome of *Cyclina sinensis* (Veneroida:Veneridae). Mitochondrial DNA. B **1(1)**: 173–174.

Dong, Y.W., H.S. Wang, G.D. Han, C.H. Ke, X. Zhan, T. Nakano and G.A. Williama. 2012. The impact of Yangtze River discharge, ocean currents and historical events on the biogeographic pattern of *Cellana toreuma* along the China coast. PLOS one **7(4)**: e36178.

Drummond, A.J., A. Rambau and M. Suchard. 2013. BEAST 1.8.0. http://beast.bio.ed.ac.uk.

Dupanloup, I., S. Schneider and L. Excoffier. 2002. A simulated annealing approach to define the genetic structure of populations. Mol. Ecol. **11(12)**: 2571–2581.

Excoffier, L. and H.E. Lischer. 2010. Arlequin suite ver 3.5: a new series of programs to perform population genetics analyses under Linux and Windows. Mol. Ecol. Resour. **10(3)**: 564–567.

Folmer, O., M. Black, W. Hoeh, R. Lutz and R. Vrijenhoek. 1994. DNA primers for amplification of mitochondrial cytochrome c oxidase subunit I from diverse metazoan invertebrates. Mol. Mar. Biol. Biotech. **3(5)**: 294–299.

Fu, Y.X. 1997. Statistical tests of neutrality of mutations against population growth, hitchhiking and background selection. Genetics **147(2)**: 915–925.

Hall, T.A. 1999. BioEdit: a user-friendly biological sequence alignment editor and analysis program for Windows 95/98/NT. Nucleic Acids Sym. **41**: 95–98.

Han, C.C., K.C. Hsu, L.S. Fang, I.M. Chang and H.D. Lin. 2019. Geographical and temporal origins of *Neocaridina* species (Decapoda: Caridea: Atyidae) in Taiwan. BMC Genetics **20(1)**: 86.

He, L., T. Mukai, C.K. Hou, Q. Ma and J. Zhang. 2015. Biogeographical role of the Kuroshio Current in the amphibious mudskipper *Periophthalmus modestus* indicated by mitochondrial DNA data. Sci. Rep. **5(1)**: 15645.

Hellberg, M.E. and V.D. Vacquie. 1999. Rapid evolution of fertilization selectivity and lysin cDNA sequences in teguline gastropods. Mol. Biol. Evol. **16(6)**: 839–848.

Hsu, K.C., H. Bor, H.D. Lin, P.H. Kuo, M.S. Tan and Y.W. Chiu. 2014. Mitochondrial DNA phylogeography of *Semisulcospira libertine* (Gastropoda: Cerithioidea: Pleuroceridae): implications the history of landform changes in Taiwan. Mol. Biol. Rep. **41(6)**: 3733–3743.

Huang, H.T., C.N. Pao, T.Y. Liao and L.L. Liu. 2020. Low genetic diversity of cultivated spotted hard clam (*Meretrix petechialis*) in Taiwan. Aquac Res. **51(7)**: 2962– 2972.

Jiang, X., Z. Ren, B. Zhao, S. Zhou, X. Ying and Y. Tang. 2020. Ameliorating Effect of Pentadecapeptide Derived from *Cyclina sinensis* on Cyclophosphamide-Induced Nephrotoxicity. Mar. Drugs **18(9)**: 462

Jiang, Y., F. Chai, Z. Wan, X. Zhang and H. Hong. 2011 Characteristics and mechanisms of the upwelling in the southern Taiwan Strait: a three-dimensional numerical model study. J. Oceanogr. **67(6)**: 699–708.

Kumar, S., G. Steecher, M. Li, C. Knyaz and K. Tamura. 2018. MEGA X: Molecular evolutionary genetics analysis across computing platforms. Mol. Biol. Evol. **35(6)**: 1547–1549.

Li, W., S. Ye, Z. Zhang, J. Tang, H. Jin, F. Huang, Z. Yang, Y. Tang, Y. Chan, G. Ding and F. Yu. 2019. Purification and characterization of a novel pentadecapeptide from protein hydrolysates of *Cyclina sinensis* and its immunomodulatory effects on RAW264.7 cells. Mar. drugs **17(1)**: 30.

Li, X., Z. Dong, B. Yan, H. Cheng, X. Meng, H. Shen and J. Li. 2010. Analysis and evaluation of nutritional components

in *Cyclina sinensis* and *Meretrix meretrix*. Food Sci. **31(3-4)**: 366–370 (in Chinese).

Liao, H.R., H.S. Yu and C.C. Su. 2008. Morphology and sedimentation of sand bodies in the tidal shelf sea of eastern Taiwan Strait. Mar. Geol. **248(3-4)**: 161–178.

Librado, P. and J. Rozas. 2009. DnaSP v5: a software for comprehensive analysis of DNA polymorphism data. Bioinformatics **25(11)**: 1451–2.

Liu, J., Q. Li, L.F. Kong and X.D. Zheng. 2011. Cryptic diversity in the pen shell *Atrina pectinata* (Bivalvia: Pinnidae): high divergence and hybridization revealed by molecular and morphological data. Mol. Ecol. **20(20)**: 4332–4345.

Liu, J., T.X. Gao, S. Wu and Y.A.P. Zhang. 2007. Pleistocene isolation in the northwestern Pacific marginal seas and limited dispersal in a marine fish, *Chelon haematocheilus* (Temminck & Schlegel, 1845). Mol. Ecol. **16(2)**: 275–288.

Marko, P.B. 2002. Fossil calibration of molecular clocks and the divergence times of geminate species pairs separated by the Isthmus of Panama. Mol. Biol. Evol. **19(11)**: 2005–2021.

Nei, M. 1987. Molecular Evolutionary Genetics. New York: Columbia University.

Nei, M. and F. Tajima. 1983. Maximum likelihood estimation of the number of nucleotide substitutions from restriction sites data. Genetics **105(1)**: 207–217.

Ni, G., Q. Li, L. Kong and H. Yu. 2014. Comparative Phylogeography in marginal seas of the northwestern Pacific. Mol. Ecol. **23(3)**: 534–548.

Ni, G., Q. Li, L. Kong and X. Zheng. 2012. Phylogeography of bivalve *Cyclina sinensis*: testing the historical glaciations and Changjiang River outflow hypotheses in Northwestern Pacific. PLOS one **7(11)**: e49487.

Othmen, A.B., M. Abhary, T. Deli, Z. Ouanes, N. Alhuwautu, N. Dimassi and L. Mansour. 2020. Lack of mitochondrial genetic structure in the endangered giant clam populations of *Tridacna maxima* (Bivalvia: Cardiidae: Tridacninae) across the Saudi Arabian coast. Acta Oceanol. Sin. **39(2)**: 28–37.

Pan, B.P., L.S. Song, W.J. Bu and J.S. Sun. 2005. Studied on genetic diversity and differentiation between two allopatric populations of *Cyclina sinensis*. Acta Hydrobiol. Sin. **29**: 372–378.

Rambaut, A., A.J. Drummond and M. Suchard. 2013. Tracer v1.6. http://tree.bio.ed.ac.uk/software/tracer/. Accessed 11 Dec.

Ramos-Onsins, S.E. and J. Rozas. 2002. Statistical properties of new neutrality tests against population growth. Mol. Biol. Evol. **19(12)**: 2092–2100.

Sanna, D., T. Lai, P. Cossu, F. Scarpa, G.L. Dedola, B. Cristo, P. Francalacci, M. Curini-Galletti, L. Mura, N. Fois, F. Maltagliati and M. Casu. 2017. Cytochrome c oxidase subunit I variability in *Ruditapes decussatus* (Veneridae) from the western Mediterranean. The European Zool. J. **84(1)**: 554–565.

Shen, K.N., B.W. Jamandre, C.C. Hsu, W.N. Tzeng and J.D. Durand. 2011. Plio-Pleistocene sea level and temperature fluctuations in the northwestern Pacific promoted speciation in the globally-distributed flathead mullet *Mugil cephalus*. BMC Evol. Biol. **11(1)**: 83.

Tajima, F. 1989. Statistical method for testing the neutral mutation hypothesis by DNA polymorphism. Genetics **123(3)**: 585–595.

Templeton, A.R. 1993. The "Eve" hypotheses: a genetic critique and reanalysis. Am. Anthropol. **95(1)**: 51–72.

Thompson, J.D., T.J. Gibson, F. Plewniak, F. Jeanmougin and D.G. Higgins. 1997. The CLUSTAL_X windows interface: flexible strategies for multiple sequence alignment aided by quality analysis tools. Nucleic Acids Res. **25(24)**: 4876–4882.

Wang, R.C. and Z.P. Wang. 2008. Science of marine shellfish culture China. Qingdao: China Ocean University Press (in Chinese).

Wang, R.C., Z.P. Wang and J.Z. Zhang. 1993. Aquaculture of marine mollusks. Qingdao: China Ocean University Press (in Chinese).

Xu, J., T.Y. Chan, L.M. Tsang and K.H. Chu. 2009. Phylogeography of the mitten crab *Eriocheir sensu stricto* in East Asia: Pleistocene isolation, population expansion and secondary contact. Mol. Phylogenet. Evol. **52(1)**: 45–56.

Xue, D.X., H.Y. Wang, T. Zhang and J.X. Liu. 2014. Population genetic structure and demographic history of *Atrina pectinata* based on mitochondrial DNA and microsatellite markers. PLOS one **9(5)**: e95436.

Yan, Y.R., K.C. Hsu, M.R. Yi, B. Li, W.K. Wang, B. Kang and H.D. Lin. 2020. Cryptic diversity of the spotted scat *Scatophagus argus* (Perciformes: Scatophagidae) in South China Sea: pre- or post-production isolation. Mar. Freshwater Res. **71(12)**: 1640–1650.

Yang, J.Q., K.C. Hsu, Z.Z. Liu, L.W. Su, P.H. Kuo, W.Q. Tang, Z.C. Zhou, D. Liu, B.L. Bao and H.D. Lin. 2016. The population history of *Garra orientalis* (Teleostei: Cyprinidae) using mitochondrial DNA and microsatellite data with approximate Bayesian computation. BMC Evol. Biol. **16(1)**: 73.

Yang, X., H. Ji, Y. Yu, J. Guan and Y. Sun. 2004. Preliminary study of the juvenile nursery of *Cyclina sinensis*. J. Shanghai Fish Univ. **13(1-3)**: 213–217 (in Chinese).

Yu, Y.S. and X.D. Zheng. 1995. The morphology and structure of the venus clam. Marine Fishery (in Chinese).

Zeng, Z.N. and F.X. Li. 1991. The study of reproductive cycle of *Cyclina sinensis*. Tropic Oceanology **10(4)**: 86–93.

Zhao, Y., Q. Li, L. Kong and Y. Mao. 2009. Genetic and morphological variation in the venus clam *Cyclina sinensis* along the coast of China. Hydrobiologia **635(1)**: 227–235.